Table II. Univariate analyses of progression-free survival time and overall survival time of patients with grade II gliomas.

Variable	No.of cases	PFS (95% CI)	p-value (log-rank)	OS (95% CI)	p-value (log-rank)
Histology					
Astrocytoma	49	3.6 (2.1-7.7)	0.08	8.3 (4.2-NR)	0.04
Oligodendroglioma/ oligoastrocytoma	23	8.3 (4.3-14.4)		11.7 (8.1-18.2)	
Age					
<40 years	38	7.0 (3.6-9.3)	0.2	NR (8.0-NR)	0.02
≥40 years	34	3.1 (1.8-8.9)		4.3 (3.9-16.3)	
IDH mutation					
Mutation	42	8.4 (3.2-10.2)	0.04	16.3 (9.6-18.2)	0.004
Wild-type	30	3.3 (1.7-7.0)		4.5 (3.9-10.0)	
Extent of removal					
Total and subtotal removal	14	10.4 (2.5-14.4)	0.1	18.3 (4.1-18.3)	0.08
Partial removal and biopsy	58	4.3 (2.3-8.3)		10.0 (5.2-16.3)	
Largest diameter of initial tumor (cm)					
<6	40	7.7 (2.3-10.4)	0.2	10.0 (8.0-NR)	0.7
≥6	32	4.3 (2.1-8.3)		10.3 (5.1-16.3)	
Initial KPS					
<80	4	0.6 (0.4-8.4)	0.01	1.7 (0.5-10.3)	0.0006
≥80	68	6.8 (3.1-8.9)		11.7 (8.0-18.2)	
MIB-1 index					
<4%	33	8.1 (2.3-8.9)	0.6	9.6 (5.1-NR)	0.6
≥4%	21	4.3 (1.8-NR)		NR (3.9-NR)	
1p/19q					
1p/19q codeletion (+)	15	6.8 (2.2-NR)	0.4	11.7 (4.3-11.7)	0.2
1p/19q codeletion (-)	45	3.6 (2.3-8.4)		8.3 (4.4-NR)	
1p					
1p deletion	24	5.8 (2.5-9.3)	0.96	11.7 (4.2-11.7)	0.9
Intact	36	4.2 (2.1-10.2)		9.6 (4.4-NR)	
19q					
19q deletion	23	7.0 (4.2-9.3)	0.5	11.7 (4.5-11.7)	0.5
Intact	37	3.1 (1.9-10.2)		8.3 (3.9-NR)	
Initial radiotherapy					
+	58	4.3 (2.9-8.9)	0.98	8.3 (5.1-18.2)	0.2
-	14	7.7 (2.5-9.1)		11.7 (4.2-16.3)	
Initial treatment					
Radiotherapy alone	16	2.9 (0.7-4.3)	0.01	4.2 (2.7-5.1)	0.0002
Chemoradiotherapy	42	8.1 (3.2-10.2)		18.2 (8.1-18.2)	

NR, PFS or median survival time is not reached; CI, confident interval.

These patients were initially treated with surgery followed by radiotherapy (22.2%) or chemoradiotherapy (58.3%). The median follow-up time for all the 72 patients was 6.4 years, and it was 7.6 years for the patients treated with chemoradiotherapy (n=42) and 4.0 years for those who underwent radiotherapy alone (n=16).

Progression-free and OS times according to clinical factors. The univariate analysis (Table II) showed that the patients with oligodendroglial tumors (n=23) had longer OS than those with diffuse astrocytoma (n=49; p=0.04). The PFS and OS were 3.6 and 8.3 years, respectively, in the patients with diffuse astrocytoma, and 8.3 and 11.7 years, respectively, in the patients with oligodendroglioma or oligoastrocytoma (Fig. 1A and B). The patients younger than 40 years (n=38) had longer OS than those who were 40 years or older (n=34; p=0.02). The PFS and median survival time of the patients in the younger age groups were 7.0 years and still not reached, respectively, whereas the PFS and OS of the patients in the older age groups were 3.1 and 4.3 years, respectively. The patients with an initial KPS score ≥80 (n=68) had significantly longer OS (p=0.0006) and PFS (p=0.01) than those with a KPS score <80 (n=4). The PFS and OS of the patients with a KPS score ≥80 were 6.8 and 11.7 years, respectively, and those of the patients with a KPS score <80 were 0.6 and 1.7 years, respectively. The patients in the total or subtotal resection (≥90% removal) groups (n=14; median age, 34.0 years) tended to have longer OS than those in the partial (<90%) removal or biopsy groups (n=58; median age, 41.0; p=0.08). The PFS and OS were 10.4 and 18.3 years, respectively, in the patients in the total or subtotal resection groups and 4.3 and 10.0 years, respectively, in the patients in the partial resection or biopsy groups. The patients who were initially treated with chemoradiotherapy after surgery showed significantly longer PFS (p=0.01) and OS (p=0.0002) than those treated with radiotherapy alone (Fig. 1C and D). The PFS and OS of the patients who were initially treated with radiotherapy after surgery (n=16) were 2.9 and 4.2 years, respectively, and the PFS and OS of the patients who were initially treated with chemoradiotherapy after surgery (n=42) were 8.1 and 18.2 years, respectively. According to MIB-1 staining index, there was no significant difference of survival between groups with cut-off point at 4, 8 and 15% in our study.

Presence of 1p/19q codeletion, 1p deletion, and 19q deletion and survival. The presence of 1p/19q deletions was determined for 25 or 26 primary resections and for 7 or 2 secondary resection samples by MLPA or FISH, respectively. The 1p/19q codeletion was observed in 15.9% (7/44) of the astrocytomas and 50% (8/16) of the oligodendroglial tumors. The OS of the patients with 1p/19q codeletion was 11.7 years, and the OS of those without 1p/19q codeletion was 8.3 years (p=0.2; Fig. 1E and F). In the patients with astrocytic tumors, the median survival time of those with 1p/19q codeletion was not reached and the OS of those without 1p/19q codeletion was 6.3 years (p=0.5). The OS of the patients with 1p/19q codeletion was 11.7 years, and the OS of those without 1p/19q codeletion was 10.3 years in the oligodendroglial tumors (p=0.5). The presence of 1p/19q codeletion, 1p deletion, or 19q deletion was not correlated with the PFS or OS time (Table II).

Table III. Mutation of *IDH1/2*.

	Diffuse astrocytoma (%)	Oligodendroglioma (%)	Oligoastrocytoma (%)
IDH1/2 mutation by sequence			
IDH1 R132H	13 (26.5)	2 (50.0)	5 (26.3)
IDH1 R132S	1 (2.0)	0 (0.0)	0 (0.0)
IDH2 R172K	1 (2.0)	0 (0.0)	0 (0.0)
Wild-type	15 (30.6)	1 (25.0)	2 (10.5)
IDH mutation by IHC			
IDH1 R132H	8 (16.3)	1 (25.0)	11 (57.9)
IDH1 R132S	0 (0.0)	0 (0.0)	0 (0.0)
Mutation (-)	11 (22.4)	0 (0.0)	1 (5.3)
Total	49 (100)	4 (100)	19 (100)
Mutation	23 (46.9)	3 (75.0)	16 (84.2)
Wild-type	26 (53.1)	1 (25.0)	3 (15.8)

IHC, immunohistochemical staining.

IDH1/2 mutations and survival in the whole series. IDH1/2 mutations were determined in 55 samples at the primary resection and 17 at the secondary resection by IHC alone for 32 cases (44.4%) and by direct sequencing in 40 cases (55.6%). IDH1/2 mutations were found in 46.9% (23/49) of the astrocytomas, 84.2% (16/19) of the oligoastrocytomas, and 75.0% (3/4) of the oligodendrogliomas (Table III).

The patients with *IDH1/2* mutations (n=42) had longer PFS (p=0.04) and OS (p=0.004) than those without IDH1/2 mutations (n=30; Table II). The PFS and OS of the patients with *IDH1/2* mutations were 8.4 and 16.3 years, respectively, and the PFS and OS of the patients without *IDH1/2* mutations were 3.3 and 4.5 years, respectively (Fig. 1G and H). The diffuse astrocytoma patients with *IDH1/2* mutations (n=23) tended to have longer survival times than those without *IDH1/2* mutations (n=26), although the difference was not significant (p=0.08). The median survival time of the diffuse astrocytoma patients with *IDH1/2* mutations was not reached and that of the diffuse astrocytoma patients without *IDH1/2* mutations was 4.4 years. The oligodendroglial tumor patients with *IDH1/2* mutations also tended to have longer, though not significant, survival times (p=0.1).

The survival of the patients with *IDH1/2* mutations and 1p/19q codeletion was longer than that of the patients with neither *IDH1/2* mutations nor 1p/19q codeletion (11.7 vs. 4.4 years, respectively), although the difference did not reach statistical significance (p=0.1). Furthermore, a combined *IDH1/2* and 1p/19q status did not correlate with the PFS and OS of the patients who were initially treated with chemoradiotherapy after surgery regardless of the histological tumor type.

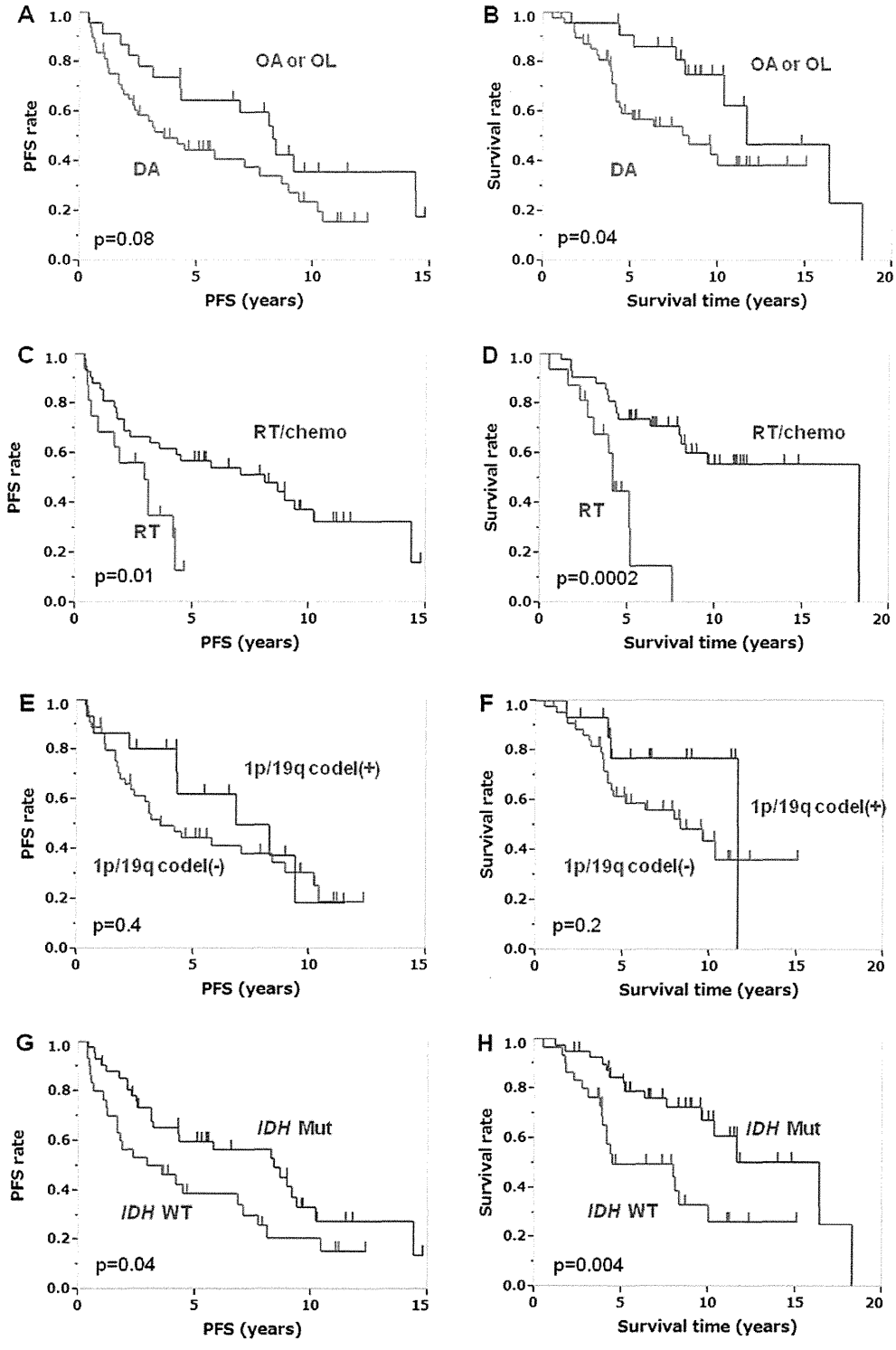

Figure 1. Kaplan-Meier survival curves of the patients with WHO grade II gliomas grouped according to genetic and clinical factors associated with overall survival (OS) and progression-free survival (PFS) by univariate analysis. The survival estimates were calculated according to the following variables: (A) PFS, diffuse astrocytoma (DA) versus oligodendroglial tumors (OA or OL); (B) OS, diffuse astrocytoma (DA) versus oligodendroglial tumors (OA or OL); (C) PFS, radiotherapy (RT) versus chemoradiotherapy (RT/chemo); (D) OS, radiotherapy (RT) versus chemoradiotherapy (RT/chemo); (E) PFS, 1p/19q codeletion (codel) (+) or (-); (F) OS, 1p/19q codeletion (codel) (+) or (-); (G) PFS, IDH1/2 mutation (mut) or wild-type (WT); and (H) OS, IDH1/2 mutation (mut) or wild-type (WT).

In the total or subtotal resection group, the patients with *IDH1/2* mutations had longer OS than those without *IDH1/2* mutations (p=0.04; Fig. 2A). The OS of the patients with *IDH1/2* mutations (n=6, 2 diffuse astrocytomas, 3 oligoastrocytomas, and 1 oligodendroglioma) was 18.2 years; to date, 5 are still alive and 1 is dead. The OS of the patients without *IDH1/2* mutations (n=8, 7 astrocytomas and 1 oligoastrocytoma) was 8.0 years. In the partial resection or biopsy group, the patients with *IDH1/2* mutations had longer OS than those without *IDH1/2* mutations in the partial resection or biopsy group (p=0.01; Fig. 2B). The OS of the patients with *IDH1/2* mutations (n=36, 21 diffuse astrocytomas, 13 oligoastrocytomas, and 2 oligodendrogliomas)

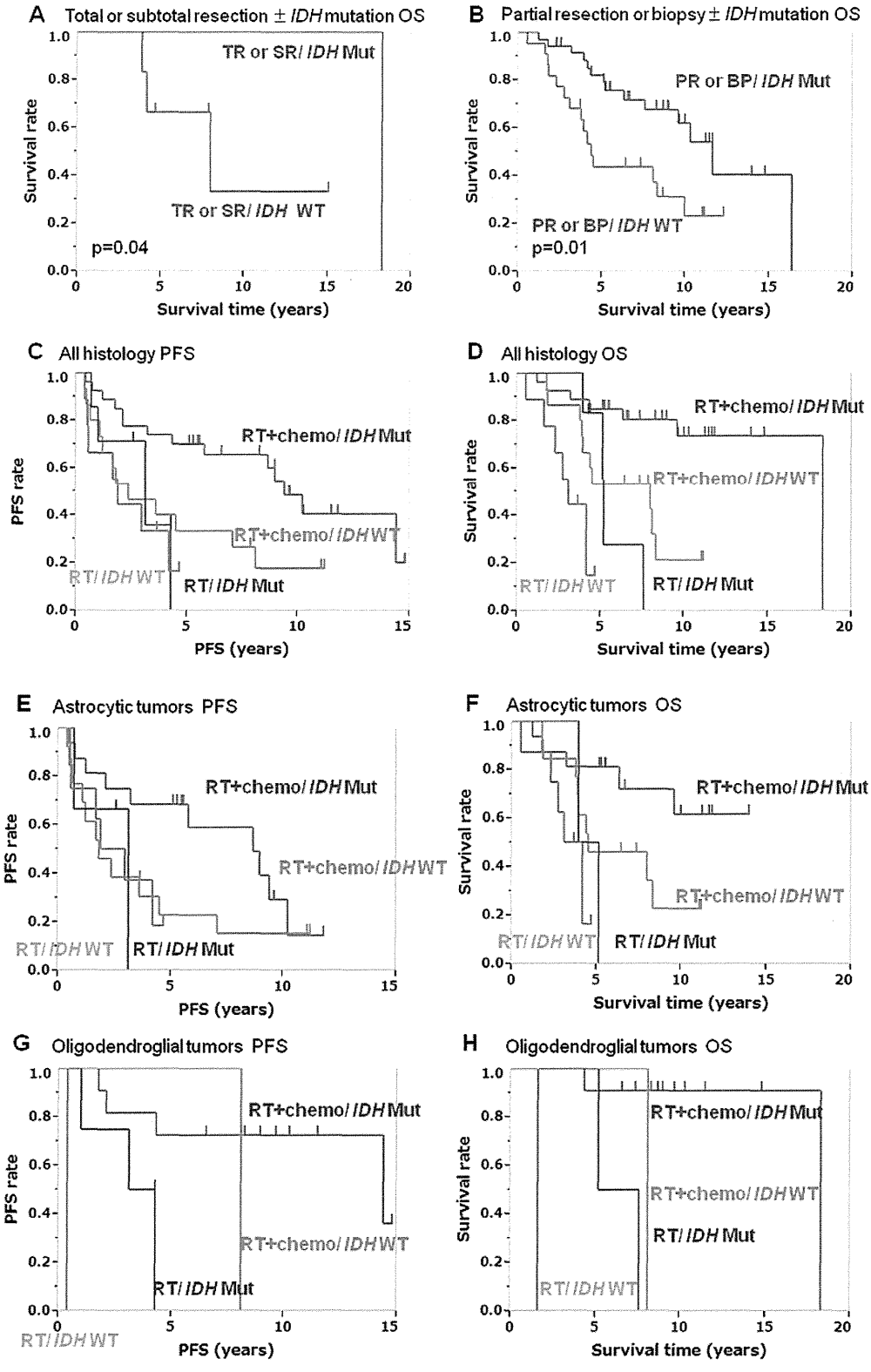

Figure 2. (A and B) Kaplan-Meier survival curves of the patients in the total or subtotal tumor resection (TR or SR) (A) and partial resection or biopsy (PR or BP) (B) groups according to the *IDH1/2* status. (C-H) Kaplan-Meier survival curves of the patients who were initially treated with radiotherapy (RT) and chemotherapy (chemo) or radiotherapy alone according to *IDH1/2* status associated with the overall survival (OS) and progression-free survival (PFS) by univariate analysis: (C) PFS of all the WHO grade II gliomas, (D) OS of all the WHO grade II gliomas, (E) PFS of the diffuse astrocytomas, (F) OS of the diffuse astrocytomas, (G) PFS of the oligodendroglial tumors, (H) OS of the oligodendroglial tumors.

was 11.7 years, and that of the patients without *IDH1/2* mutations in these groups (n=22, 19 diffuse astrocytomas, 2 oligoastrocytomas, and 1 oligodendroglioma) was 4.4 years.

IDH1/2 mutations and survival in the patients who underwent chemoradiotherapy after surgery. Among the grade II glioma patients who were initially treated with chemoradiotherapy

Table IV. PFS and OS in patients with radiotherapy or chemoradiotherapy according to IDH1/2 status.

Variable		No. of cases	PFS (95% CI)	OS (95% CI)
All grade II gliomas				
RT+chemo	Mut (+)	27	9.3 (4.3-NA)[a,b]	18.2 (9.6-18.2)[c,d]
RT+chemo	Mut (-)	15	2.3 (0.6-7.0)[a-,b]	8.0 (3.8-8.3)[c,d]
RT only	Mut (+)	7	3.1 (0.7-4.3)[b]	5.1 (3.9-7.5)[b,d,e]
RT only	Mut (-)	9	1.9 (0.4-4.2)	3.1 (0.5-4.2)[b,e]
Diffuse astrocytoma				
RT+chemo	Mut (+)	16	8.6 (2.1-10.2)[f]	NR (6.3-NR)[g,h]
RT+chemo	Mut (-)	13	1.8 (0.6-4.5)[f]	4.5 (3.8-NR)[g,h]
RT only	Mut (+)	3	3.1 (0.7-3.1)[f]	4.5 (3.9-5.1)[h]
RT only	Mut (-)	8	2.4 (0.5-NR)	3.6 (0.5-NR)
Oligodendroglioma/oligoastrocytoma				
RT+chemo	Mut (+)	11	14.4 (2.1-NR)[e]	18.2 (NR)[a]
RT+chemo	Mut (-)	2	8.1 (NR)[e]	8.1 (NR)[a]
RT only	Mut (+)	4	3.7 (1.0-4.3)[e,i]	6.3 (5.1-7.5)[a,i]
RT only	Mut (-)	1	0.4 (NR)[i]	1.6 (NR)[i]

NR, PFS or median survival time is not reached; CI, confident interval; RT, radiotherapy; chemo, chemotherapy; mut, mutation. [a]p=0.02; [b]p=0.01; [c]p=0.004; [d]p=0.008; [e]p=0.03; [f]p=0.1; [g]p=0.06; [h]p=0.07; [i]p=0.05.

Table V. Multivariate analyses of PFS and OS of patients with all grade II gliomas.

Variable	No. of cases	PFS hazard ratio (95% CI)	PFS p-value (Cox)	OS hazard ratio (95% CI)	OS p-value (Cox)
Histology					
Diffuse astrocytoma	49	1	0.1	1	0.02
Oligodendroglioma/ oligoastrocytoma	23	0.576 (0.262-1.186)		0.290 (0.086-0.815)	
IDH mutation					
Wild-type	31	1	0.08	1	0.01
Mutation	41	0.558 (0.289-1.068)		0.365 (0.155-0.819)	
Age (years)					
≥40	34	1	0.5	1	0.02
<40	38	0.802 (0.440-1.460)		0.400 (0.175-0.877)	
Extent of removal					
Partial removal and biopsy	58	1	0.1	1	0.2
Total and subtotal removal	14	0.556 (0.222-1.217)		0.463 (0.107-1.403)	
Initial KPS					
<80	4	1	0.01	1	0.0002
≥80	68	0.179 (0.063-0.640)		0.045 (0.011-0.198)	

CI, confident interval.

after surgery, those with *IDH1/2* mutations had significantly longer PFS and OS than those without *IDH1/2* mutations (PFS: p=0.02, OS: p=0.004; Fig. 2C and D; Table IV).

An important finding is that the patients who were initially treated with chemoradiotherapy after surgery and had *IDH1/2* mutations showed significantly longer PFS and OS than those

Table VI. Multivariate analyses of PFS and OS of patients with all grade II gliomas with radiotherapy ± chemotherapy.

Variable	No. of cases	PFS hazard ratio (95% CI)	PFS p-value (Cox)	OS hazard ratio (95% CI)	OS p-value (Cox)
Histology					
Diffuse astrocytoma	40	1	0.2	1	0.2
Oligodendroglioma/ Oligoastrocytoma	18	0.549 (0.209-1.290)		0.490 (0.133-1.445)	
IDH mutation					
Wild-type	24	1	0.05	1	0.01
Mutation	34	0.467 (0.215-0.999)		0.316 (0.117-0.793)	
Age (years)					
≥40	28	1	0.5	1	0.5
<40	30	0.758 (0.362-1.559)		0.745 (0.300-1.808)	
Extent of removal					
Partial removal and biopsy	47	1	0.03	1	0.08
Total and subtotal removal	11	0.364 (0.118-0.918)		0.356 (0.080-1.120)	
Initial treatment					
Radiotherapy alone	16	1	0.04	1	0.002
Chemoradiotherapy	42	0.408 (0.182-0.948)		0.198 (0.073-0.529)	

CI, confident interval.

treated with radiotherapy alone with *IDH1/2* mutations. The PFS and OS of the patients with *IDH1/2* mutations who were initially treated with chemoradiotherapy after surgery (n=27) were 9.3 and 18.2 years, respectively, and the PFS and OS of those treated with radiotherapy alone with *IDH1/2* mutations (n=7) were 3.1 and 5.1 years, respectively (PFS, p=0.01; OS, p=0.008). In the oligodendroglial tumors, the PFS and OS of the patients with *IDH1/2* mutations who were initially treated with chemoradiotherapy (n=11) were 14.4 and 18.2 years, respectively, and the PFS and OS of those treated with radiotherapy alone with *IDH1/2* mutations (n=4) were 3.7 and 6.3 years, respectively (PFS: p=0.03, OS: p=0.02; Fig. 2G and H). Similar tendencies, although not reaching statistical significance, were observed in the astrocytic tumors (PFS: p=0.1, OS: p=0.07; Fig. 2E and F).

The *IDH1/2* status had no impact on the PFS of all the grade II glioma or diffuse astrocytoma patients who underwent radiotherapy alone. No significant difference in PFS was observed between the radiotherapy and chemoradiotherapy groups in the grade II glioma patients without *IDH1/2* mutations. Chemoradiotherapy did not prolong the PFS of the patients without *IDH1/2* mutations in the astrocytic and oligodendroglial tumors.

Multivariate analysis. Oligodendroglial tumors (hazard ratio (HR)=0.29, p=0.02), age <40 years (HR=0.40, p=0.02), initial KPS ≥80 (HR=0.045, p=0.0002), and *IDH1/2* mutations (HR=0.37, p=0.01) were favorable prognostic factors for OS time, as determined by the multivariate analysis, of the 72 patients included in the study (Table V). The *IDH1/2* mutation status was not a prognostic factor for PFS when all the patients were considered, including those who did not undergo initial radiotherapy or chemotherapy (p=0.08). In contrast, total or subtotal tumor resection (HR=0.36, p=0.03), chemoradiotherapy (HR=0.41, p=0.04), and *IDH1/2* mutations (HR=0.47, p=0.05) were favorable prognostic factors for PFS, as determined by the multivariate analysis, of the patients who were initially treated with radiotherapy or chemoradiotherapy (Table VI). Histological appearance was not a prognostic marker for PFS in this series (p=0.2) compared with *IDH1/2* mutations (p=0.05).

Discussion

WHO grade III and IV astrocytomas with *IDH1/2* mutations have more favorable prognoses than those with wild-type *IDH1/2* (17). *IDH1/2* mutations, 1p/19q codeletion, and *MGMT* promoter methylation are pivotal prognostic factors in anaplastic oligodendroglial tumors treated with radiotherapy or chemoradiotherapy (EORTC 26951) (27). However, the impact of *IDH1/2* mutations and/or 1p/19q codeletion as biomarkers in grade II gliomas remains controversial. The present study was therefore aimed at identifying prognostic and/or predictive factors in grade II gliomas.

The presence of IDH1/2 mutations is a favorable prognostic marker for OS. The results of the univariate analysis revealed that the presence of *IDH1/2* mutations was a prognostic factor of longer OS (p=0.004) and PFS (p=0.04) in the entire patient cohort and among the patients who underwent with or without radiation therapy after initial surgery with or without chemotherapy. The multivariate analysis revealed that the presence of

IDH1/2 mutations was associated with prolonged PFS (p=0.05) and OS (p=0.01) in the patients who initially underwent radiotherapy with or without chemotherapy. Our results suggest that *IDH1/2* mutations may be involved in the response to genotoxic therapy, such as radiotherapy or chemotherapy, and may act as a prognostic factor for chemotherapy or radiotherapy in grade II gliomas. There are currently increasing numbers of reports showing that *IDH1/2* mutations are prognostic markers for several malignancies, including grade II gliomas. Houillier *et al* (19) reported that the presence of *IDH1/2* mutations is a significant prognostic marker for OS and chemosensitivity in low-grade glioma patients who were initially treated with temozolomide (TMZ) before any other treatment except surgery. Hartmann *et al* (16) reported that the *IDH1* mutation was a prognostic factor for PFS and OS in grade II glioma patients who underwent radiotherapy or chemotherapy after surgery. In our study, the presence of *IDH1/2* mutations was demonstrated by multivariate analysis to be a favorable prognostic factor (p=0.01) for OS but not a prognostic marker for PFS (p=0.08) in whole cohort, which included 14 patients who did not receive initial radiotherapy. Our finding that *IDH1/2* status did not affect PFS was in line with the findings reported by Hartmann *et al* (16) or Houillier *et al* (16,19), who showed that *IDH1* mutations did not affect the PFS in grade II glioma patients who did not receive radiotherapy or chemotherapy alone after surgery. Kim *et al* (21) and Mukasa *et al* (22) reported that the presence of *IDH1/2* mutations was not a prognostic factor for the survival of patients with low-grade glioma in univariate or multivariate analyses. The treatment of those patients was not fully described in their reports.

The presence of IDH1/2 mutations is a predictive marker for PFS in the grade II glioma patients treated with chemoradiotherapy. The patients who were initially treated with chemoradiotherapy after surgery showed significantly longer OS (p=0.0002) and PFS (p=0.01) than those treated with radiotherapy alone in our study. Chemoradiotherapy significantly prolonged PFS and OS compared with radiotherapy alone in all the grade II gliomas with *IDH1/2* mutations (p=0.01 and 0.0008, respectively), diffuse astrocytoma (p=0.1 and 0.07, respectively), and oligodendroglial tumors (p=0.03 and 0.02, respectively) in the univariate analysis. Chemoradiotherapy was shown by multivariate analysis (p=0.04) to significantly prolong the PFS of grade II glioma patients carrying *IDH1/2* mutations who underwent radiotherapy with or without concomitant chemotherapy (p=0.04). In contrast, there were no differences in PFS between the radiotherapy and chemoradiotherapy groups among the grade II glioma patients without *IDH1/2* mutations in the univariate analysis. PFS did not differ by *IDH1/2* status in the grade II glioma patients who underwent radiotherapy alone. However, the present study was limited by the small number of samples and the differences in the follow-up periods between the radiation and chemoradiotherapy groups (4 and 7.6 years, respectively). A prospective study including a larger patient cohort is required to obtain conclusive evidence that the presence of *IDH1/2* mutations is a predictive marker for chemoradiotherapy in grade II gliomas. Nonetheless, our results suggest that *IDH1/2* mutation is a predictive marker for chemoradiotherapy in grade II glioma patients and indicate that these patients may benefit from concurrent chemotherapy and radiotherapy compared with patients who do not carry *IDH1/2* mutations.

Mutations in *IDH1/2* result in the acquisition of new enzymatic activity that enables the NADPH-dependent reduction of α-ketoglutarate to 2-hydroxyglutarate, and the mutation confers oncogenic properties (28). *IDH1* mutations are early events in the development of astrocytomas and oligodendrogliomas (11). Another possible function of *IDH1/2* mutations is the dominant-negative inhibition of the oxidative decarboxylation of isocitrate as a result of the formation of a wild-type/mutant heterodimer (29). Cellular IDH1 levels are associated with the protection from apoptosis and cell death after exposure to reactive oxygen species or ultraviolet B-induced phototoxicity and *IDH1/2* functions in cellular defense reactions (30). Glioma cells with *IDH1/2* mutations may be vulnerable to irradiation and chemotherapeutic agents, which might explain why *IDH1/2* mutations could be a predictive and prognostic marker for grade II gliomas in patients receiving chemoradiotherapy. Our findings warrant a prospective large-scale clinical study addressing the efficacy of chemoradiotherapy in grade II glioma patients in association with *IDH1/2* status.

Grade II glioma patients with wild-type IDH1/2 have poor prognoses even after total resection. The extent of resection of tumors has been reported to be significantly associated with survival and recurrence of disease in low-grade glioma patients (9,31). In our study, the patients in the total or subtotal resection (≥90% removal) group tended to have longer survival times than the patients in the partial (<90% removal) or biopsy group (p=0.08). The patients without *IDH1/2* mutations had shorter OS than those with *IDH1/2* mutations in the total and subtotal resection groups (p=0.04) and in the partial and biopsy groups (p=0.01). Although the number of patients examined was small, we believe that this is a very important finding and that it indicates that patients without *IDH1/2* mutations may require more intensive treatment, such as chemoradiotherapy, even after total resection of the tumor.

1p/19q codeletion is not a prognostic factor. In our study, the OS and PFS in the diffuse astrocytomas with 1p/19q codeletion tended to be longer than those in the patients without 1p/19q codeletion, but the difference did not reach statistical significance. Furthermore, no significant differences were observed between the grade II glioma patients with regard to 1p/19q status. Prior studies reported that the presence of the 1p/19q codeletion was significantly associated with longer OS in low-grade gliomas (12,13,15,21,32). On the other hand, Houillier *et al* and Mukasa *et al* (19,22) reported that loss of 1p/19q was not a sensitive prognostic biomarker. Ichimura *et al* and Vogazianou *et al* reported that total 1p/19q loss is rare and that when present, it is associated with longer survival than other 1p/19q changes in adult gliomas independent of pathological diagnosis (14,15). Deletion of 1p or 19q was determined mainly by FISH analysis in our study, and this technique cannot discriminate between total and partial 1p/19q deletion, which might explain the discrepancy in the results.

Clinicopathological factors in grade II gliomas. The multivariate analysis showed that age ≥40 years (p=0.02), astrocytic tumors (p=0.02), initial KPS <80 (p=0.0002), and wild-type *IDH1/2* (p=0.01) were unfavorable prognostic factors in our series. These results are generally in line with previous reports

showing that older age, astrocytic histology, presence of neurologic deficits before surgery, largest tumor diameter, and tumors crossing the midline were important unfavorable prognostic factors for survival in adult patients with low-grade gliomas (5-9).

In conclusion, the multivariate analysis showed that age <40 years, oligodendroglial tumors, initial KPS ≥80, and *IDH1/2* mutations were favorable prognostic factors for survival of the grade II glioma patients. The presence of *IDH1/2* mutations was a prognostic factor for grade II glioma patients with radiotherapy. Furthermore, it is a predictive factor of response to chemoradiotherapy in grade II gliomas. Patients carrying *IDH1/2* mutations may benefit more from concurrent chemotherapy and radiotherapy compared with those without *IDH1/2* mutations.

Acknowledgements

We thank all the doctors, nurses and medical staff in National Cancer Center Hospital who attended to the glioma patients in these 20 years. This study was supported by National Cancer Center Research and Development Fund no. 23-A-49.

References

1. Louis DN, Ohgaki H, Wiestler OD, Cavenee WK, Burger PC, Jouvet A, Scheithauer BW and Kleihues P: The 2007 WHO classification of tumours of the central nervous system. Acta Neuropathol 114: 97-109, 2007.
2. Bauman G, Fisher B, Watling C, Cairncross JG and Macdonald D: Adult supratentorial low-grade glioma: long-term experience at a single institution. Int J Radiat Oncol Biol Phys 75: 1401-1407, 2009.
3. van den Bent MJ, Afra D, de Witte O, Ben Hassel M, Schraub S, Hoang-Xuan K, Malmstrom PO, Collette L, Pierart M, Mirimanoff R and Karim AB: Long-term efficacy of early versus delayed radiotherapy for low-grade astrocytoma and oligodendroglioma in adults: the EORTC 22845 randomised trial. Lancet 366: 985-990, 2005.
4. Shaw EG, Wang M, Coons S, Brachman D, Buckner JC, Stelzer K, Barger G, Brown PD, Gilbert MR and Mehta MP: Final report of Radiation Therapy Oncology Group (RTOG) protocol 9802: radiation therapy (RT) versus RT + procarbazine, CCNU, and vincristine (PCV) chemotherapy for adult low-grade glioma (LGG). J Clin Oncol (ASCO Meeting abst) 26: 2006, 2008.
5. Bauman G, Lote K, Larson D, Stalpers L, Leighton C, Fisher B, Wara W, MacDonald D, Stitt L and Cairncross JG: Pretreatment factors predict overall survival for patients with low-grade glioma: a recursive partitioning analysis. Int J Radiat Oncol Biol Phys 45: 923-929, 1999.
6. Chang EF, Smith JS, Chang SM, Lamborn KR, Prados MD, Butowski N, Barbaro NM, Parsa AT, Berger MS and McDermott MM: Preoperative prognostic classification system for hemispheric low-grade gliomas in adults. J Neurosurg 109: 817-824, 2008.
7. Pignatti F, van den Bent M, Curran D, Debruyne C, Sylvester R, Therasse P, Afra D, Cornu P, Bolla M, Vecht C and Karim AB: Prognostic factors for survival in adult patients with cerebral low-grade glioma. J Clin Oncol 20: 2076-2084, 2002.
8. Schiff D, Brown PD and Giannini C: Outcome in adult low-grade glioma: the impact of prognostic factors and treatment. Neurology 69: 1366-1373, 2007.
9. Smith JS, Chang EF, Lamborn KR, Chang SM, Prados MD, Cha S, Tihan T, Vandenberg S, McDermott MW and Berger MS: Role of extent of resection in the long-term outcome of low-grade hemispheric gliomas. J Clin Oncol 26: 1338-1345, 2008.
10. Smith JS, Alderete B, Minn Y, Borell TJ, Perry A, Mohapatra G, Hosek SM, Kimmel D, O'Fallon J, Yates A, *et al*: Localization of common deletion regions on 1p and 19q in human gliomas and their association with histological subtype. Oncogene 18: 4144-4152, 1999.
11. Watanabe T, Nobusawa S, Kleihues P and Ohgaki H: IDH1 mutations are early events in the development of astrocytomas and oligodendrogliomas. Am J Pathol 174: 1149-1153, 2009.
12. Smith JS, Perry A, Borell TJ, Lee HK, O'Fallon J, Hosek SM, Kimmel D, Yates A, Burger PC, Scheithauer BW and Jenkins RB: Alterations of chromosome arms 1p and 19q as predictors of survival in oligodendrogliomas, astrocytomas, and mixed oligoastrocytomas. J Clin Oncol 18: 636-645, 2000.
13. Mariani L, Deiana G, Vassella E, Fathi AR, Murtin C, Arnold M, Vajtai I, Weis J, Siegenthaler P, Schobesberger M and Reinert MM: Loss of heterozygosity 1p36 and 19q13 is a prognostic factor for overall survival in patients with diffuse WHO grade 2 gliomas treated without chemotherapy. J Clin Oncol 24: 4758-4763, 2006.
14. Ichimura K, Vogazianou AP, Liu L, Pearson DM, Backlund LM, Plant K, Baird K, Langford CF, Gregory SG and Collins VP: 1p36 is a preferential target of chromosome 1 deletions in astrocytic tumours and homozygously deleted in a subset of glioblastomas. Oncogene 27: 2097-2108, 2008.
15. Vogazianou AP, Chan R, Backlund LM, Pearson DM, Liu L, Langford CF, Gregory SG, Collins VP and Ichimura K: Distinct patterns of 1p and 19q alterations identify subtypes of human gliomas that have different prognoses. Neurooncology 12: 664-678, 2010.
16. Hartmann C, Hentschel B, Tatagiba M, Schramm J, Schnell O, Seidel C, Stein R, Reifenberger G, Pietsch T, von Deimling A, Loeffler M and Weller M: Molecular markers in low-grade gliomas: predictive or prognostic? Clin Cancer Res 17: 4588-4599, 2011.
17. Yan H, Parsons DW, Jin G, McLendon R, Rasheed BA, Yuan W, Kos I, Batinic-Haberle I, Jones S, Riggins GJ, *et al*: IDH1 and IDH2 mutations in gliomas. N Engl J Med 360: 765-773, 2009.
18. Balss J, Meyer J, Mueller W, Korshunov A, Hartmann C and von Deimling A: Analysis of the IDH1 codon 132 mutation in brain tumors. Acta Neuropathol 116: 597-602, 2008.
19. Houillier C, Wang X, Kaloshi G, Mokhtari K, Guillevin R, Laffaire J, Paris S, Boisselier B, Idbaih A, Laigle-Donadey F, *et al*: IDH1 or IDH2 mutations predict longer survival and response to temozolomide in low-grade gliomas. Neurology 75: 1560-1566, 2010.
20. Metellus P, Coulibaly B, Colin C, de Paula AM, Vasiljevic A, Taieb D, Barlier A, Boisselier B, Mokhtari K, Wang XW, *et al*: Absence of IDH mutation identifies a novel radiologic and molecular subtype of WHO grade II gliomas with dismal prognosis. Acta Neuropathol 120: 719-729, 2010.
21. Kim YH, Nobusawa S, Mittelbronn M, Paulus W, Brokinkel B, Keyvani K, Sure U, Wrede K, Nakazato Y, Tanaka Y, *et al*: Molecular classification of low-grade diffuse gliomas. Am J Pathol 177: 2708-2714, 2010.
22. Mukasa A, Takayanagi S, Saito K, Shibahara J, Tabei Y, Furuya K, Ide T, Narita Y, Nishikawa R, Ueki K and Saito N: Significance of IDH mutations varies with tumor histology, grade, and genetics in Japanese glioma patients. Cancer Sci 103: 587-592, 2012.
23. Camelo-Piragua S, Jansen M, Ganguly A, Kim JC, Louis DN and Nutt CL: Mutant IDH1-specific immunohistochemistry distinguishes diffuse astrocytoma from astrocytosis. Acta Neuropathol 119: 509-511, 2010.
24. Hartmann C, Meyer J, Balss J, Capper D, Mueller W, Christians A, Felsberg J, Wolter M, Mawrin C, Wick W, *et al*: Type and frequency of IDH1 and IDH2 mutations are related to astrocytic and oligodendroglial differentiation and age: a study of 1,010 diffuse gliomas. Acta Neuropathol 118: 469-474, 2009.
25. Franco-Hernandez C, Martinez-Glez V, de Campos JM, Isla A, Vaquero J, Gutierrez M, Casartelli C and Rey JA: Allelic status of 1p and 19q in oligodendrogliomas and glioblastomas: multiplex ligation-dependent probe amplification versus loss of heterozygosity. Cancer Genet Cytogenet 190: 93-96, 2009.
26. Schouten JP, McElgunn CJ, Waaijer R, Zwijnenburg D, Diepvens F and Pals G: Relative quantification of 40 nucleic acid sequences by multiplex ligation-dependent probe amplification. Nucleic Acids Res 30: e57, 2002.
27. van den Bent MJ, Dubbink HJ, Marie Y, Brandes AA, Taphoorn MJ, Wesseling P, Frenay M, Tijssen CC, Lacombe D, Idbaih A, *et al*: IDH1 and IDH2 mutations are prognostic but not predictive for outcome in anaplastic oligodendroglial tumors: a report of the European Organization for Research and Treatment of Cancer Brain Tumor Group. Clin Cancer Res 16: 1597-1604, 2010.

28. Dang L, White DW, Gross S, Bennett BD, Bittinger MA, Driggers EM, Fantin VR, Jang HG, Jin S, Keenan MC, *et al*: Cancer-associated IDH1 mutations produce 2-hydroxyglutarate. Nature 462: 739-744, 2009.
29. Zhao S, Lin Y, Xu W, Jiang W, Zha Z, Wang P, Yu W, Li Z, Gong L, Peng Y, *et al*: Glioma-derived mutations in IDH1 dominantly inhibit IDH1 catalytic activity and induce HIF-1alpha. Science 324: 261-265, 2009.
30. Reitman ZJ and Yan H: Isocitrate dehydrogenase 1 and 2 mutations in cancer: alterations at a crossroads of cellular metabolism. J Natl Cancer Inst 102: 932-941, 2010.
31. Ahmadi R, Dictus C, Hartmann C, Zurn O, Edler L, Hartmann M, Combs S, Herold-Mende C, Wirtz CR and Unterberg A: Long-term outcome and survival of surgically treated supratentorial low-grade glioma in adult patients. Acta Neurochir 151: 1359-1365, 2009.
32. Daniels TB, Brown PD, Felten SJ, Wu W, Buckner JC, Arusell RM, Curran WJ, Abrams RA, Schiff D and Shaw EG: Validation of EORTC prognostic factors for adults with low-grade glioma: a report using intergroup 86-72-51. Int J Radiat Oncol Biol Phys 81: 218-224, 2011.

J Neurol (2012) 259:1698–1705
DOI 10.1007/s00415-011-6402-5

ORIGINAL COMMUNICATION

Fractional anisotropy in the centrum semiovale as a quantitative indicator of cerebral white matter damage in the subacute phase in patients with carbon monoxide poisoning: correlation with the concentration of myelin basic protein in cerebrospinal fluid

Takaaki Beppu · Shunrou Fujiwara · Hideaki Nishimoto · Atsuhiko Koeda · Shinsuke Narumi · Kiyoshi Mori · Kuniaki Ogasawara · Makoto Sasaki

Received: 23 October 2011 / Accepted: 26 December 2011 / Published online: 19 January 2012

Abstract Carbon monoxide (CO) poisoning leads to demyelination of cerebral white matter (CWM) fibers, causing chronic neuropsychiatric symptoms. To clarify whether fractional anisotropy (FA) from diffusion tensor imaging in the centrum semiovale can depict demyelination in the CWM during the subacute phase after CO inhalation, we examined correlations between FA in the centrum semiovale and myelin basic protein (MBP) in cerebrospinal fluid. Subjects comprised 26 adult CO-poisoned patients ≤60 years old. MBP concentration was examined for all patients at 2 weeks after CO inhalation. The mean FA of the centrum semiovale bilaterally at 2 weeks was also examined for all patients and 21 age-matched healthy volunteers as controls. After these examinations, the presence of chronic symptoms was checked at 6 weeks after CO poisoning. Seven patients displayed chronic symptoms, of whom six showed abnormal MBP concentrations. The remaining 19 patients presented no chronic symptoms and no abnormal MBP concentrations, with MBP concentrations undetectable in 16 patients. The MBP concentration differed significantly between patients with and without chronic symptoms. The mean FA was significantly lower in patients displaying chronic symptoms than in either patients without chronic symptoms or controls. After excluding the 16 patients with undetectable MBP concentrations, a significant correlation was identified between MBP concentration and FA in ten patients. The present results suggest that FA in the centrum semiovale offers a quantitative indicator of the extent of demyelination in damaged CWM during the subacute phase in CO-poisoned patients.

Keywords Carbon monoxide poisoning · Cerebral white matter fiber · Demyelination · Diffusion tensor imaging · Fractional anisotropy · Myelin basic protein

Abbreviation

CNS	Central nervous system
CSF	Cerebrospinal fluid
CO	Carbon monoxide
COHb	Carboxyhemoglobin
DNS	Delayed neuropsychiatric sequelae
DTI	Diffusion tensor imaging
FA	Fractional anisotropy
ADC	Apparent diffusion coefficient
GCS	Glasgow coma scale
MBP	Myelin basic protein

T. Beppu (✉) · S. Fujiwara · H. Nishimoto · K. Ogasawara
Department of Neurosurgery, Iwate Medical University, Uchimaru 19-1, Morioka 020-8505, Japan
e-mail: tbeppu@iwate-med.ac.jp

T. Beppu
Department of Hyperbaric Medicine, Iwate Medical University, Uchimaru 19-1, Morioka 020-8505, Japan

A. Koeda
Department of Psychiatry, Iwate Medical University, Uchimaru 19-1, Morioka 020-8505, Japan

S. Narumi
Department of Neurology, Iwate Medical University, Uchimaru 19-1, Morioka 020-8505, Japan

K. Mori
Iwate Prefectural Advanced Critical Care and Emergency Center, Morioka, Japan

M. Sasaki
Advanced Medical Research Center, Iwate Medical University, Morioka, Japan

MRI Magnetic resonance imaging
ROI Region of interest
T2WI T2-weighted magnetic resonance imaging

Introduction

Approximately 30% of patients surviving acute carbon monoxide (CO) poisoning display various chronic neuropsychiatric symptoms [31, 32]. Of these, approximately two-thirds demonstrate persistent neurological symptoms from the acute phase to the chronic phase. The remaining one-third show delayed neuropsychiatric sequelae (DNS), which are recurrent neuropsychiatric symptoms occurring after an interval of apparent normality ("lucid interval;" mean duration 22 days) following apparent recovery from acute symptoms [6, 33]. Animal experiments and some clinical studies have led to the hypothesis that damage after CO poisoning results from complicated mechanisms due to CO-mediated toxicity: mitochondrial oxidative stress in the central nervous system (CNS) following CO-induced tissue hypoxia [35]; perivascular oxidative stress mediated by intravascular neutrophil activation [26]; and alteration of myelin basic protein (MBP), a major myelin component in the CNS, due to lipid peroxygenation leading to auto-immunological demyelination of CNS [24, 25]. Auto-immunological demyelination induces further inflammation in the cerebral white matter (CWM) [31]. Gray matter structures, such as the cerebral cortex, basal ganglia and hippocampus, must be damaged by severe hypoxia, since these structures display higher cellular activity and higher oxygen requirements than white matter structures and are more vulnerable to oxygen deprivation [29]. However, damage in the CWM is seen in patients both with and without damage to gray matter structures, and the severity of CWM damage appears to correlate with prognosis in CO-poisoned patients [15, 34].

Assessment of CWM damage caused by CO poisoning in the acute or subacute phase contributes to predictions of progress to DNS and prognosis of chronic symptoms, and appropriate triage of patients with CO poisoning for observation and treatment. Additional quantitative and objective examinations are desirable for assessment of CWM damage after CO poisoning. However, no universally accepted severity scale in routine examinations, such as level of consciousness or carboxyhemoglobin concentration, is available for assessing CWM damage caused by CO poisoning. This is because clinical features are largely affected by the degree of cellular hypoxia resulting from binding of CO to myoglobin rather than hemoglobin and may be markedly affected by various conditions before admission, such as the duration before hospitalization and the care provided before hospitalization [7, 12, 20]. As one of mechanisms for damage in CWM is auto-immunological demyelination, measuring the MBP concentration in the cerebrospinal fluid (CSF) has recently been proposed as an indicator for the extent of CWM damage after CO poisoning [11, 14]. However, detection of MBP using a lumbar tap is a highly invasive procedure and only indicates white-matter damage somewhere within the entire CNS. A less-invasive, objective and quantitative examination that could be used in place of measuring MBP is therefore desired. Diffusion tensor imaging (DTI), a magnetic resonance imaging (MRI) sequence, is potentially more sensitive for detecting demyelination in CWM. Among various quantitative parameters such as apparent diffusion coefficient (ADC) and eigenvalues derived from DTI, fractional anisotropy (FA) has been recognized as the most useful for evaluating the integrity of CWM fibers [2]. Indeed, FA is frequently used for evaluating the extent of damaged CWM fibers in patients with demyelinating diseases such as multiple sclerosis [1, 27]. CO poisoning causes damage in various regions of the CWM, but the centrum semiovale has been considered a region more responsible for chronic neuropsychiatric symptoms after CO poisoning than other regions [4, 10, 19, 22]. Herein, we measured FA from DTI at the centrum semiovale in CO-poisoned patients, and evaluated the correlation between the FA and concentration of MBP in the CSF. This study aimed to clarify whether FA in the centrum semiovale offers a quantitative indicator of the extent of demyelination in damaged CWM during the subacute phase in CO-poisoned patients.

Methods

Patients

All study protocols were approved by the Ethics Committee of Iwate Medical University, Morioka, Japan. Patients recruited to this study were admitted to Iwate Medical University Hospital between April 2008 and February 2011. Entry criteria for this study were: age $\geq$20 but $\leq$60 years in patients who had suffered from CO poisoning caused by a fire or charcoal burning; performance of DTI and measurement of MBP concentration according to the protocol in this study; no past history of brain disorders, including surgical operation, irradiation, stroke, infection or demyelinating disease; and provision of written informed consent to participate. Diagnosis was based on present history of exposure to CO and presence of acute neurological symptoms such as impairment of consciousness and headache on admission. After excluding patients

who did not meet the entry criteria, 26 patients were enrolled. Mean duration from the scene of CO exposure to arrival at our institute was 5.0 h (range 0.3–81 h). All patients were treated with hyperbaric oxygenation therapy (HBO_2) (60 min of 100% oxygen inhalation via mask at 2.8 atmospheres absolute) started within 24 h of admission. HBO_2 was continued with a single daily session for a week excluding the weekend. HBO_2 was further continued for 4–8 weeks in cases with persistent symptoms. If DNS occurred, HBO_2 was restarted and continued until 2 months after CO exposure. HBO_2 was discontinued upon patient request or when symptoms were sufficiently improved. Duration of HBO_2 administration for all patients ranged from 1 to 60 sessions (mean 12 sessions). The day of CO inhalation was defined as day 1 in this study.

Measurement of MBP concentration in CSF

MBP concentration in the CSF was examined using a lumbar tap at 2 weeks after CO poisoning (between day 12 and day 16) for all patients. Obtained CSF was frozen at −20°C within 1 h after lumbar tap, then the frozen CSF was transported on dry ice to an outside laboratory (SRL, Tokyo, Japan). MBP in the CSF was assayed and measured using a MBP ELISA kit (Cosmic Corp., Tokyo, Japan) immediately after arrival at the laboratory. If the assay was delayed for a long time, frozen CSF was stored at −80°C. An abnormal MBP concentration was defined as ≥102 pg/ml. When the level of MBP was below the limit of detection, the result from the laboratory was reported as MBP ≤40 pg/ml.

DTI

For all patients, DTI was also performed at 2 weeks (between day 12 and day 16) using a 3.0-T whole-body scanner (GE Yokogawa Medical Systems, Tokyo, Japan) and 8-channel coil. Measurements of FA and ADC were performed using data from DTI (repetition time, 10,000 ms; echo time, 62 ms; matrix 128 × 128; field of view, 240 × 240 mm; 4 mm thickness with 1.5 mm gap; 6 motion-probing gradient directions; b value, 1,000 s/mm^2). The region of interest (ROI) was manually placed in the bilateral centrums semiovale in the CWM on non-diffusion-weighted images (Fig. 1). FA and ADC were measured bilaterally at the centrum semiovale, using free MRIcro software (http://www.cabiatl.com/mricro/). The FA and ADC for each subject were determined as the mean of values measured twice by the same investigator (S.F.), who was blinded to clinical data. The second measurement was performed 1 week after the first test, using a different randomized order of measurements from the first test.

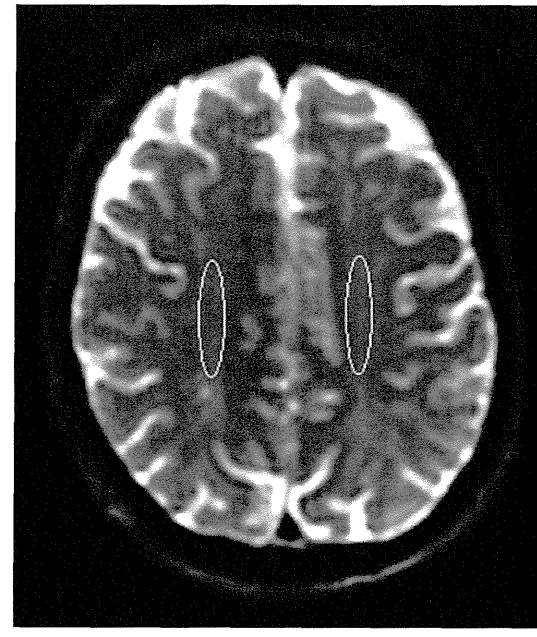

Fig. 1 Measurements of FA and ADC value at the centrum semiovale in a patient (case 7 in group S). Regions of interest (ROIs) were placed bilaterally on the centrum semiovale in non-diffusion-weighted image

Finally, the mean FA and mean ADC values for the right and left centrum semiovale were calculated and defined as absolute values for each subject. The same procedures described above were performed for 21 age-matched healthy volunteers as controls (18 men, 3 women; mean age 41 ± 10 years, range 22–56 years).

Observation of symptoms

Neurological symptoms were continuously observed for 6 weeks after admission using routine neurological examinations. Patients were assigned to one of two groups according to clinical behavior at 6 weeks (day 40–44) after CO poisoning: group S, patients displaying neuropsychiatric symptoms; group A, patients showing asymptomatic status. Group S included both patients with symptoms persisting for 6 weeks and patients with DNS. DNS was defined as recurrent symptoms after apparent improvement of acute symptoms followed by a lucid interval. General intellectual function was also estimated using the mini-mental state examination (MMSE) [9] at 6 weeks after CO exposure. We defined the normal range, borderline range and dementia according to MMSE scores as ≥27, ≤26 but ≥22, and ≤21, respectively. When scores were considered borderline, patients with educational background ≥9 years and evidence of obvious personality change according to interviews with family members were diagnosed with dementia.

Statistical analyses

We statistically compared differences in mean age among group S, group A and controls using the Mann-Whitney U test. The incidence of abnormal ($\geq$102 pg/ml) MBP concentration was compared between the two patient groups (group S and group A) using the χ^2 for independence test. Mean FA and mean ADC values among two patients groups and controls were compared using the Mann-Whitney U test. Intra-operator reliability for all absolute FA and ADC values was evaluated according to classification of the intra-class correlation coefficient (ICC) [21]. For ICC(1,1) and ICC(1,k) as intra-operator reliability, agreement of all absolute values between the first and second tests was analyzed for right and left lesions using one-factor analysis of variance. After excluding patients showing undetectable concentrations of MBP ($\leq$40 pg/ml), the correlation between MBP and mean FA value was estimated using Spearman's correlation coefficient by rank test. Statistical significance was established at the $p < 0.05$ level in all analyses.

Results

A total of 51 patients were admitted to our institute for treatment of CO poisoning between April 2008 and February 2011. After excluding 25 patients who did not meet the entry criteria for this study, a total of 26 patients (24 men, 2 women; mean age 40.1 $\pm$ 11.4 years) were enrolled. All patient data are summarized in Table 1. In 19 (73%) of 26 patients, acute symptoms resolved completely within 4 days after admission, and no neuropsychiatric symptoms were present at 6 weeks from CO-inhalation (group A). The remaining seven patients (27%) displayed chronic neuropsychiatric symptoms at 6 weeks (group S), including four patients with continuous persistence of symptoms for 6 weeks and three patients exhibiting DNS

Table 1 Summary of all patients

Case	Group	Age	Etiology	COHb (%)	GCS	MBP (pg/ml)	Mean FA	Mean ADC	Main symptom at 6 weeks	MMSE score
1	S	29	Suicide	24.8	11	252	0.345	0.622	Dementia (persistent)	23
2	S	57	Suicide	25.1	10	176	0.344	0.548	Parkinsonism (persistent)	27
3	S	38	Suicide	1.5	6	468	0.239	0.494	Apallic syndrome (persistent)	NS
4	S	55	Suicide	39.7	3	376	0.346	0.548	Dementia (persistent)	16
5	S	56	Suicide	13.5	11	130	0.338	0.584	Akinetic mutism (DNS)	NS
6	S	29	Suicide	3.6	14	99	0.353	0.498	Parkinsonism (DNS)	28
7	S	48	Suicide	28.6	6	110	0.317	0.565	Dementia (DNS)	23
1	A	22	Suicide	20.5	15	52.8	0.488	0.492	None	29
2	A	31	Suicide	47.3	13	40.6	0.354	0.494	None	30
3	A	22	Suicide	9.3	12	63.6	0.447	0.555	None	30
4	A	47	Heating	33.3	14	$\leq$40	0.441	0.496	None	30
5	A	44	Heating	13.7	15	$\leq$40	0.388	0.528	None	30
6	A	26	Suicide	1.9	15	$\leq$40	0.395	0.504	None	30
7	A	47	Heating	22.6	14	$\leq$40	0.393	0.551	None	29
8	A	28	Suicide	19.2	15	$\leq$40	0.440	0.521	None	30
9	A	41	Suicide	2.7	11	$\leq$40	0.381	0.487	None	30
10	A	55	Heating	14.0	13	$\leq$40	0.366	0.504	None	30
11	A	35	Suicide	25.3	8	$\leq$40	0.425	0.497	None	30
12	A	56	Suicide	12.2	15	$\leq$40	0.395	0.501	None	30
13	A	36	Suicide	44.1	12	$\leq$40	0.398	0.513	None	30
14	A	34	Suicide	31.0	12	$\leq$40	0.394	0.530	None	30
15	A	57	Heating	40.1	13	$\leq$40	0.400	0.541	None	30
16	A	32	Suicide	19.3	10	$\leq$40	0.358	0.509	None	30
17	A	34	Suicide	38.6	5	$\leq$40	0.406	0.535	None	30
18	A	36	Suicide	23.5	10	$\leq$40	0.358	0.520	None	30
19	A	48	Suicide	44.0	6	$\leq$40	0.352	0.539	None	30

COHb and GCS indicate results of the initial examination

COHb carboxyhemoglobin, *GCS* Glasgow coma scale, *NS* no study performed because of unconsciousness

after apparent improvement of acute symptoms followed by a lucid interval. DNS in three patients occurred after DTI and measurement of MBP on day 21 in case 5, day 19 in case 6 and day 18 in case 7. Mean age was 45 ± 12 years in group S, 38 ± 11 years in group A and 41 ± 10 years in controls. No significant differences in age were found between groups S and A ($p = 0.24$), between group S and controls ($p = 0.51$), or between group A and controls ($p = 0.40$).

In the seven patients in sroup S, six showed abnormal MBP concentrations (≥102 pg/ml), and one patient showed a level of 99 pg/ml. None of the 19 patients in group A showed abnormal concentrations of MBP, with 16 patients showing undetectable concentrations of MBP (≤40 pg/ml). The incidence of an abnormal MBP levels was statistically different between groups P and A ($p < 0.001$). MBP concentrations for the four patients with persistent symptoms in group S, for the three patients with DNS in group S and for the three patients in group A were more than ≥150 pg/ml, around 100 pg/ml and around 50 pg/ml, respectively (Table 1).

Table 2 shows ranges and means of FA and ADC for each group. The range of FA for group S slightly overlapped that for group A, but differed markedly from that for controls. Ranges of FA for group A and controls were similar. The mean FA for group S was significantly lower than those for group A ($p < 0.001$) and controls ($p < 0.001$), whereas no significant difference was found between group A and controls ($p = 0.57$) (Fig. 2a). In Fig. 2a, individual mean FA values of the three patients with DNS were not obviously different from those of the four patients with persistent symptoms in group S. Group S patients were clearly differentiated from group A patients at a cutoff of 0.353 (100% sensitivity, 94.7% specificity) and from controls at a cutoff of 0.360 (100% sensitivity, 100% specificity). On the other hand, the range of ADC in each group was similar, and the mean ADC did not differ significantly among any of the three groups (Fig. 2b). Intra-operator reliability for absolute FA was classified as "almost perfect" for the centrum semiovale bilaterally; ICC(1,1) and ICC(1,*k*) were 0.88 and 0.93 for the right side, and 0.95 and 0.98 for the left side, respectively. Intra-operator reliability for absolute ADC was also classified as "almost perfect" for bilateral centrum semiovale; ICC(1,1) and ICC(1,*k*) were 0.98 and 0.99 for the right side, and 0.91 and 0.95 for the left side, respectively.

After excluding 16 patients showing undetectable levels (≤40 pg/ml), the ten remaining patients (all patients in groups S and 3 patients in group A) showed a strong correlation between the mean FA and MBP ($r = -0.79$, $p = 0.02$) (Fig. 3).

Discussion

Ide et al. [11] have documented that MBP concentration in patients with DNS showed marked elevation around 2 weeks after CO poisoning, peaking at around 30 days.

Table 2 Range and mean value of FA and ADC for each group

	FA		ADC ($\times 10^{-3}$ mm^2/s)	
	Range	Mean	Range	Mean
Group S	0.239–0.353	0.326 ± 0.040	0.494–0.622	0.551 ± 0.045
Group A	0.352–0.447	0.395 ± 0.029	0.487–0.601	0.517 ± 0.021
Controls	0.363–0.445	0.400 ± 0.027	0.472–0.580	0.517 ± 0.023

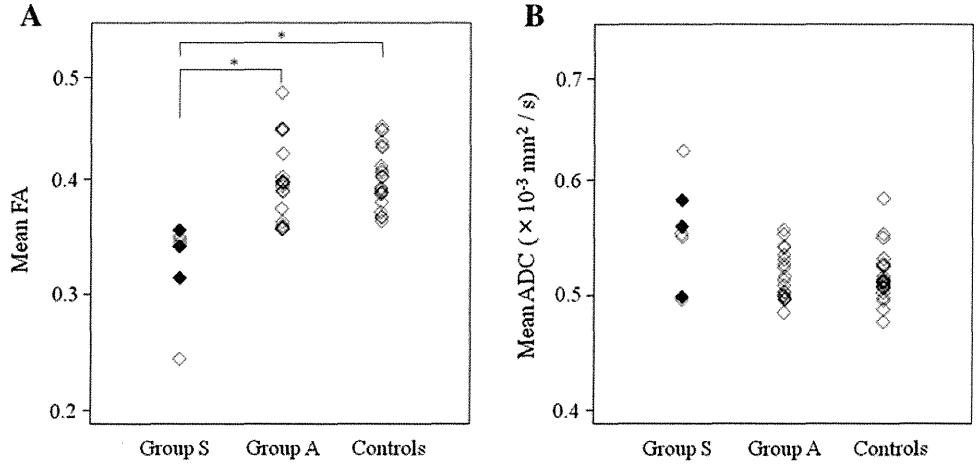

Fig. 2 Differences of mean FA (**a**) and mean ADC (**b**) values in the centrum semiovale bilaterally among group S, group A and controls. In group S, *black and white squares* represent patients with DNS and persistent symptoms, respectively (*$p < 0.001$).

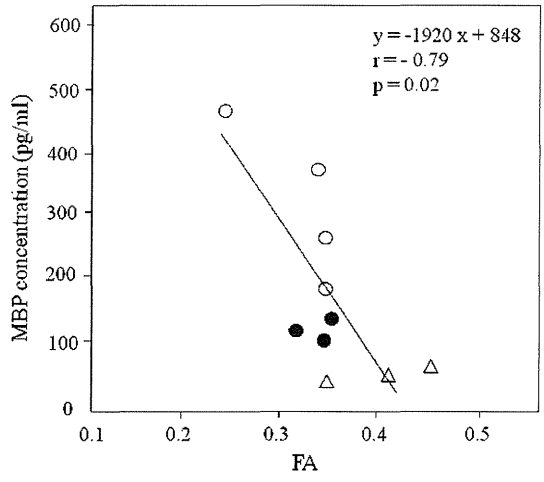

Fig. 3 Correlation between FA and MBP concentration in ten patients showing MBP concentration >40 pg/ml. *White circle*, patient with persistent chronic symptoms in group S; *black circle*, patient with DNS in group S; *triangle*, patient in group A

The timing for MBP measurements in the present study was thus established at 2 weeks (between day 12 and day 16) after admission. As a result, the incidence of abnormal MBP concentration was significantly higher in patients with chronic neuropsychiatry symptoms (group S) than in patients without chronic symptoms (group A) or controls. These results suggest that patients in group S certainly suffered from demyelinating changes somewhere in the CWM and support the theory that chronic neuropsychiatric symptoms after CO intoxication result from progressive demyelination in the CWM [24, 25]. The MBP concentration in case 6 was slightly lower (99 pg/ml) than the abnormal level, but the patient displayed akinetic mutism compatible with DNS at 1 week after measurement of MBP. The concentration of MBP in this patient might have been on the way to reaching abnormal levels, as demyelination of CWM in patients with DNS has been considered to undergo gradual progression during the lucid interval [13]. MBP concentrations of DNS patients were between those of patients with persistent symptoms in group S and those of patients in group A (Table 1; Fig. 3). These findings may indicate that demyelination begins to progress during the lucid interval before DNS. Although measuring MBP concentrations thus offers a useful indicator for assessing the extent of demyelination due to CO poisoning, detection of MBP using a lumbar tap is a highly invasive procedure and only indicates white-matter damage somewhere within the CNS.

Neuroimaging is minimally invasive and can visualize any region in the CWM. T2-weighted imaging (T2WI) often depicts abnormalities in the CWM in CO-poisoned patients. However, the interpretation of findings from routine MRI is difficult, as hyperintense foci in the CWM on T2WI can represent various progressive histological changes, including vasogenic edema, multiple necrosis, extensive axonal destruction and/or demyelination without axonal destruction [4, 12]. We therefore performed DTI in the same period as detection of MBP, since DTI is potentially more sensitive for assessing the extent of demyelinating changes in the CWM than other MRI sequences. As progressive reduction of FA values with age has been reported [5], we compared patients <60 years old with age-matched controls in this study. The finding of no significant difference in mean age among groups S, group A and controls suggests a negligible contribution of aging to FA values in this study. Previous reports have documented damage in various regions of the CWM after CO poisoning [8, 18, 28]. Indeed, some studies have reported correlations between FA values in various regions of the CWM in the chronic phase and cognitive dysfunction among CO-poisoned patients with DNS [16, 23, 30]. However, the centrum semiovale in the CWM has been suggested as a key region responsible for chronic neurological symptoms [4, 10, 19, 22]. A study using DTI at various phases after CO poisoning has also shown that FA in the centrum semiovale changes in parallel with cognitive impairments or neurological symptoms [17]. Based on these reports, we placed the ROI on the centrum semiovale to measure FA and ADC from DTI. As a result, mean FA for group S presenting with chronic neuropsychiatric symptoms was significantly lower than that for group A presenting with no chronic symptoms or that for controls consisting of healthy volunteers, whereas no significant difference was evident between group A and controls. In contrast, mean ADC did not differ significantly among the three groups. FA must be more sensitive for detecting CWM damage than ADC. Furthermore, these findings suggest that white matter fibers in the centrum semiovale were demyelinated in the subacute phase (2 weeks after poisoning) in CO-poisoned patients presenting with chronic symptoms. Notably, reductions in FA, suggestive of demyelination, were already present in the centrum semiovale before the recurrence of symptoms in the three patients with DNS. The reliability of this finding is supported by the result that MBP concentrations in DNS patients showed greater increases than those in group A patients at 2 weeks. These findings indicate the possibility of using FA in the centrum semiovale as an appropriate examination for predicting DNS during the lucid interval.

Our pilot study of DTI for CO-poisoned patients showed that FA enables representation of damage to white matter fibers in the centrum semiovale of patients with chronic neuropsychiatric symptoms [3]. That report, however, failed to demonstrate any correlation between FA in the centrum semiovale and MBP concentration, presumably because of the small sample size. Although subject criteria

were more strictly established in the present study than in our previous investigation, the greater number of subjects in this study allow us to show a linear correlation between FA and MBP in ten patients showing MBP concentrations >40 pg/ml. This finding validated the use of the centrum semiovale to represent various demyelinated lesions in the CWM, and FA in the centrum semiovale obviously offers a quantitative indicator of demyelination in CO-poisoned patients with chronic neuropsychiatric symptoms.

Some limitations must be considered in the interpretation of the study results. First, FA in the centrum semiovale may not strictly mirror the amount of demyelination in the whole CWM, although FA in the centrum semiovale correlated with MBP concentration. In group S, FA values in the centrum semiovale of the three DNS patients were not clearly different from those of the four patients with persistent symptoms (Fig. 2a), whereas MBP seemed to allow differentiation between subgroups in group S (around 100 pg/ml in patients with DNS and ≥150 pg/ml in patients with persistent chronic symptoms). This discrepancy might hypothetically be explained if demyelinated lesions in patients with persistent symptoms vary more than those in DNS patients. FA measured in this study suggests the magnitude of demyelination in the centrum semiovale, whereas MBP concentration not only indicates the magnitude, but also the width of demyelination in the whole CNS. We think that FA in the centrum semiovale cannot allow differentiation of the severity of CWM damage among subjects including patients with DNS and those with persistent symptoms. Second, the chronic neuropsychiatric symptoms seen after CO poisoning may not be solely attributable to demyelinating changes in fibers of the centrum semiovale. However, knowing to the focus on the region of the CWM is obviously very useful when evaluating the extent of CO-induced CWM damage using neuroimaging. We considered that the centrum semiovale represents the main region of damage and should be the focus of attention on neuroimaging in the subacute phase after CO poisoning [10]. Third, the sample size in this study was still small, with markedly fewer subjects in group S than in group A. The small number of DNS patients resulted in difficulties with statistical comparisons between subgroups in group S and other groups. However, the small sample size resulted from the strict entry criteria for this study. Furthermore, we did not select subjects with any bias other than the criteria established for this study. Indeed, percentages for patients with and without chronic symptoms in this study were in agreement with the results of previous reports [6, 33]. Fourth, findings in this study cannot be applied to patients over 60 years old. In senior patients, FA values may be overestimated as aging may lead to reduced FA values.

Conclusions

This is the first report to find that FA in the CWM correlates with MBP concentrations in the CSF during the subacute phase in CO-poisoned patients. The identification of a significant negative correlation between FA in the centrum semiovale and MBP concentration validates the concept that the centrum semiovale can reveal various demyelinated lesions in the CWM and that FA in the centrum semiovale offers a quantitative indicator of demyelination in CO-poisoned patients with chronic neuropsychiatric symptoms.

Acknowledgments This study was supported in part by a Grant-in-Aid for Scientific Research (C) and for the Strategic Medical Science Research Center for Advanced Medical Science Research from the Ministry of Science, Education, Sports and Culture, Japan.

Conflicts of interest None.

References

1. Bammer R, Augustin M, Strasser-Fuchs S, Seifert T, Kapeller P, Stollberger R, Ebner F, Hartung HP, Fazekas F (2000) Magnetic resonance diffusion tensor imaging for characterizing diffuse and focal white matter abnormalities in multiple sclerosis. Magn Reson Med 44:583–591
2. Beaulieu C (2002) The basis of anisotropic water diffusion in the nervous system—a technical review. NMR Biomed 15:435–455
3. Beppu T, Nishimoto H, Ishigaki D, Fujiwara S, Yoshida T, Oikawa H, Kamada K, Sasaki M, Ogasawara K (2010) Assessment of damage to cerebral white matter fiber in the subacute phase after carbon monoxide poisoning using fractional anisotropy in diffusion tensor imaging. Neuroradiology 52:735–743
4. Chang KH, Han MH, Kim HS, Wie BA, Han MC (1992) Delayed encephalopathy after acute carbon monoxide intoxication: MR imaging features and distribution of cerebral white matter lesions. Radiology 184:117–122
5. Charlton RA, Barrick TR, McIntyre DJ, Shen Y, O'Sullivan M, Howe FA, Clark CA, Morris RG, Markus HS (2006) White matter damage on diffusion tensor imaging correlates with age-related cognitive decline. Neurology 66:217–222
6. Choi IS (1983) Delayed neurologic sequelae in carbon monoxide intoxication. Arch Neurol 40:433–435
7. Ernst A, Zibrak JD (1998) Carbon monoxide poisoning. N Engl J Med 339:1603–1608
8. Fan HC, Wang AC, Lo CP, Chang KP, Chen SJ (2009) Damage of cerebellar white matter due to carbon monoxide poisoning: a case report. Am J Emerg Med 27(757):e755–e757
9. Folstein MF, Folstein SE, McHugh PR (1975) "Mini-mental state". A practical method for grading the cognitive state of patients for the clinician. J Psychiatr Res 12:189–198
10. Fujiwara S, Beppu T, Nishimoto H, Sanjo K, Koeda A, Mori K, Kudo K, Sasaki M, Ogasawara K (2011) Detecting damaged regions of cerebral white matter in the subacute phase after carbon

monoxide poisoning using voxel-based analysis with diffusion tensor imaging. Neuroradiology. doi:10.1007/s00234-011-0958-8
11. Ide T, Kamijo Y (2008) Myelin basic protein in cerebrospinal fluid: a predictive marker of delayed encephalopathy from carbon monoxide poisoning. Am J Emerg Med 26:908–912
12. Jain K (2009) Carbon monoxide and other tissue poisons. In: Jain KK (ed) Textbook of hyperbaric medicine, 5th edn. Hogrefe and Huber Publisher, Massachusetts, pp 43–133
13. Kado H, Kimura H, Murata T, Itoh H, Shimosegawa E (2004) Carbon monoxide poisoning: two cases of assessment by magnetization transfer ratios and 1H-MRS for brain damage. Radiat Med 22:190–194
14. Kamijo Y, Soma K, Ide T (2007) Recurrent myelin basic protein elevation in cerebrospinal fluid as a predictive marker of delayed encephalopathy after carbon monoxide poisoning. Am J Emerg Med 25:483–485
15. Lapresle J, Fardeau M (1967) The central nervous system and carbon monoxide poisoning. II. Anatomical study of brain lesions following intoxication with carbon monixide (22 cases). Prog Brain Res 24:31–74
16. Lin WC, Lu CH, Lee YC, Wang HC, Lui CC, Cheng YF, Chang HW, Shih YT, Lin CP (2009) White matter damage in carbon monoxide intoxication assessed in vivo using diffusion tensor MR imaging. AJNR Am J Neuroradiol 30:1248–1255
17. Lo CP, Chen SY, Chou MC, Wang CY, Lee KW, Hsueh CJ, Chen CY, Huang KL, Huang GS (2007) Diffusion-tensor MR imaging for evaluation of the efficacy of hyperbaric oxygen therapy in patients with delayed neuropsychiatric syndrome caused by carbon monoxide inhalation. Eur J Neurol 14:777–782
18. O'Donnell P, Buxton PJ, Pitkin A, Jarvis LJ (2000) The magnetic resonance imaging appearances of the brain in acute carbon monoxide poisoning. Clin Radiol 55:273–280
19. Parkinson RB, Hopkins RO, Cleavinger HB, Weaver LK, Victoroff J, Foley JF, Bigler ED (2002) White matter hyperintensities and neuropsychological outcome following carbon monoxide poisoning. Neurology 58:1525–1532
20. Prockop LD, Chichkova RI (2007) Carbon monoxide intoxication: an updated review. J Neurol Sci 262:122–130
21. Shrout PE, Fleiss JL (1979) Intraclass correlations: uses in assessing rater reliability. Psychol Bull 86:420–428
22. Sohn YH, Jeong Y, Kim HS, Im JH, Kim JS (2000) The brain lesion responsible for parkinsonism after carbon monoxide poisoning. Arch Neurol 57:1214–1218
23. Terajima K, Igarashi H, Hirose M, Matsuzawa H, Nishizawa M, Nakada T (2008) Serial assessments of delayed encephalopathy after carbon monoxide poisoning using magnetic resonance spectroscopy and diffusion tensor imaging on 3.0T system. Eur Neurol 59:55–61
24. Thom SR (1990) Carbon monoxide-mediated brain lipid peroxidation in the rat. J Appl Physiol 68:997–1003
25. Thom SR, Bhopale VM, Fisher D, Zhang J, Gimotty P (2004) Delayed neuropathology after carbon monoxide poisoning is immune-mediated. Proc Natl Acad Sci USA 101:13660–13665
26. Thom SR, Bhopale VM, Han ST, Clark JM, Hardy KR (2006) Intravascular neutrophil activation due to carbon monoxide poisoning. Am J Respir Crit Care Med 174:1239–1248
27. Tievsky AL, Ptak T, Farkas J (1999) Investigation of apparent diffusion coefficient and diffusion tensor anisotrophy in acute and chronic multiple sclerosis lesions. AJNR Am J Neuroradiol 20:1491–1499
28. Uchino A, Hasuo K, Shida K, Matsumoto S, Yasumori K, Masuda K (1994) MRI of the brain in chronic carbon monoxide poisoning. Neuroradiology 36:399–401
29. Valk J, van der Knaap MS (1992) Toxic encephalopathy. AJNR Am J Neuroradiol 13:747–760
30. Vila JF, Meli FJ, Serqueira OE, Pisarello J, Lylyk P (2005) Diffusion tensor magnetic resonance imaging: a promising technique to characterize and track delayed encephalopathy after acute carbon monoxide poisoning. Undersea Hyperb Med 32:151–156
31. Weaver LK (2009) Clinical practice. Carbon monoxide poisoning. N Engl J Med 360:1217–1225
32. Weaver LK, Hopkins RO, Chan KJ, Churchill S, Elliott CG, Clemmer TP, Orme JF Jr, Thomas FO, Morris AH (2002) Hyperbaric oxygen for acute carbon monoxide poisoning. N Engl J Med 347:1057–1067
33. Weaver LK, Hopkins RO, Elliott G (1999) Carbon monoxide poisoning. N Engl J Med 340:1290 Author reply 1292
34. Zagami AS, Lethlean AK, Mellick R (1993) Delayed neurological deterioration following carbon monoxide poisoning: MRI findings. J Neurol 240:113–116
35. Zhang J, Piantadosi CA (1992) Mitochondrial oxidative stress after carbon monoxide hypoxia in the rat brain. J Clin Invest 90:1193–1199

International Journal of
Radiation Oncology
biology • physics

www.redjournal.org

Clinical Investigation: Central Nervous System Tumor

Clinical Value of [^{11}C]Methionine PET for Stereotactic Radiation Therapy With Intensity Modulated Radiation Therapy to Metastatic Brain Tumors

Kazuhiro Miwa, MD,*,† Masayuki Matsuo, MD,§ Jun Shinoda, MD,*,† Tatsuki Aki, MD,*,† Shingo Yonezawa, MD,*,† Takeshi Ito, MD,‡ Yoshitaka Asano, MD,*,† Mikito Yamada, MD,‡ Kazutoshi Yokoyama, MD,‡ Jitsuhiro Yamada, MD,‡ Hirohito Yano, MD,‖ and Toru Iwama, MD‖

**Chubu Medical Center for Prolonged Traumatic Brain Dysfunction, Kizawa Memorial Hospital, Minokamo, Gifu, Japan; †Department of Clinical Brain Sciences, Gifu University Graduate School of Medicine, Minokamo, Gifu, Japan; ‡Department of Neurosurgery, Kizawa Memorial Hospital, Minokamo, Gifu, Japan; §Department of Radiation Oncology, Kizawa Memorial Hospital, Minokamo, Gifu, Japan; and ‖Department of Neurosurgery, Gifu University Graduate School of Medicine, Gifu, Japan*

Received May 16, 2011, and in revised form Feb 15, 2012. Accepted for publication Feb 16, 2012

Summary

We investigated the impact of [^{11}C]methionine-positron emission tomography (MET-PET) for SRT-IMRT in brain metastasis. In 42 tumors, gross tumor volume was defined by magnetic resonance imaging (MRI) with MET-PET. MET uptake values in tumors before and after SRT-IMRT were evaluated and compared with MRI examination. Consequently, the differences in MET uptake between the pre-SRT-IMRT group and post-SRT-IMRT group were statistically significant, irrespective of MRI

Purpose: This study investigated the clinical impact of ^{11}C-labeled methionine-positron emission tomography (MET-PET) for stereotactic radiation therapy with intensity modulated radiation therapy (SRT-IMRT) in metastatic brain tumors.

Methods and Materials: Forty-two metastatic brain tumors were examined. All tumors were treated with SRT-IMRT using a helical tomotherapy system. Gross tumor volume (GTV) was defined and drawn on the stereotactic magnetic resonance (MR) image, taking into account the respective contributions of MR imaging and MET-PET. Planning target volume (PTV) encompassed the GTV-PET plus a 2-mm margin. SRT-IMRT was performed, keeping the dose for PTV at 25-35 Gy in 5 fractions. The ratio of the mean value of MET uptake to the contralateral normal brain (L/N ratio) was plotted for the PTV prior to SRT-IMRT, at 3 months following SRT-IMRT, and at 6 months following SRT-IMRT. Tumor characteristic changes of MET uptake before and after SRT-IMRT were evaluated quantitatively, comparing them with MRI examination.

Results: Mean ± SD L/N ratios were 1.95 ± 0.83, 1.18 ± 0.21, and 1.12 ± 0.25 in the pre-SRT-IMRT group, in the 3 months post-SRT-IMRT group, and in the 6 months post-SRT-IMRT group, respectively. Differences in the mean L/N ratio between the pre-SRT-IMRT group and the 3-month post-SRT-IMRT group and between the pre-SRT-IMRT group and the 6 month post-SRT-IMRT group were statistically significant, irrespective of MRI examination.

Conclusions: We showed examples of metastatic lesions demonstrating significant decreases in MET uptake following SRT-IMRT. MET-PET seems to have a potential role in providing additional information, although MRI remains the gold standard for diagnosis and follow-up after SRT-IMRT. The present study is a preliminary approach, but to more clearly define the impact

Reprint requests to: Kazuhiro Miwa, MD, Department of Neurosurgery, Chubu Medical Center for Prolonged Traumatic Brain Dysfunction, Kizawa Memorial Hospital, 630 Shimokobi, Kobi-cho, Minokamo, Gifu 505-0034, Japan. Tel: +81-574-24-2233; Fax: +81-574-24-2230; E-mail: doctor.3@jasmine.ocn.ne.jp

Conflict of interest: none.

Int J Radiation Oncol Biol Phys, Vol. 84, No. 5, pp. 1139–1144, 2012
0360-3016/$ - see front matter
doi:10.1016/j.ijrobp.2012.02.032

examination. MET-PET may have a potential role in providing additional information for the diagnosis and follow-up after SRT-IMRT.

of PET-based radiosurgical assessment, further experimental and clinical analyses are required.

Introduction

The higher specificity and sensitivity of ^{11}C-labeled methionine-positron emission tomography (MET-PET) in imaging of brain tumors has been demonstrated in previous studies and may be helpful for detection of the tumor and for assessment of radiosurgical treatment (1-3). Recently, a technique has been developed that allows routine integration of PET in stereotactic radiosurgery (4-7).

This study investigated the clinical impact of MET-PET for stereotactic radiation therapy with intensity modulated radiation therapy (SRT-IMRT) in brain metastases. In this preliminary study, MET-PET images were imported into the planning software for SRT-IMRT dosimetry, and the final target volume was defined and drawn on the stereotactic magnetic resonance (MR) image. Finally, we investigated the characteristic changes of MET-PET in tumors for monitoring after SRT-IMRT and evaluated differences between the image changes on MET-PET compared to those on MRI.

Methods and Materials

Patient population

Twenty patients with a total of 42 metastatic brain tumors were treated with SRT-IMRT at Kizawa Memorial Hospital between February 2008 and May 2010. Patients and metastases characteristics are shown in Tables 1 and 2. Computed tomography, MRI, and MET-PET were performed separately within 1 week in all 20 patients for SRT-IMRT treatment planning. Eight patients had multiple metastatic brain tumors. Karnofsky performance status levels were between 70% and 100% (mean, 80%). Our institutional ethics committee approved the study protocol, and all patients provided written informed consent.

PET methods

The PET scanner was an Advance NXi Imaging System (General Electric Yokokawa Medical System, Hino-shi, Tokyo), which provides 35 transaxial images at 4.25-mm intervals. The in-plane spatial resolution (full width at half-maximum) was 4.8 mm, and scans were performed in standard 2-dimensional mode. Before emission scans were performed, a 3-min transmission scan was performed to correct photon attenuation,using a ring source containing ^{68}Ge. A dose of 7.0 MBq/kg MET was injected intravenously into the cubital vein within 1 min. Emission scans were acquired for 30-min, beginning 5 min after MET injection. During MET-PET data acquisition, head motion was continuously monitored using laser beams projected onto ink markers drawn over the forehead skin and was corrected as necessary.

MRI methods

MRI for radiation treatment planning was performed using 1.5-T equipment (Signa Horizon LX; General Electric, Waukesha, WI). Acquisitions were made using a standard head coil without rigid immobilization. An axial, 3D gradient echo T1-weighted sequence with contrast medium (0.1 mmol/kg body weight, gadolinium-diethylenetriamine-pentaacetic acid [Gd-DTPA]; Magnevist, Schering, Berlin, Germany), and 2.0-mm slice thicknesses were acquired from the foramen magnum to the vertex, perpendicular to the main magnetic field.

Treatment protocol

Image registrations were performed using Syntegra software (Philips Medical System), using a combination of automatic and manual methods. Quantitative accuracy of the mutual information registration was evaluated and approved by 3 observers, (ie, a neurosurgeon, a radiation oncologist, and a nuclear medicine specialist). The 3 observers delineated gross target volume (GTV) by using MRI. Planning began with a separate analysis of each stereotactic imaging modality. A 3D volumetric contour was drawn on stereotactic MR images, corresponding to the area of Gd-DTPA enhancement. Then, the stereotactic PET images are analyzed independently by the 3 observers together. Abnormal PET signal suitable for target definition corresponded to areas of increased tracer uptake compared with the surrounding normal brain. A 3D volumetric PET contour delineating these areas was drawn on a visual basis and projected onto the corresponding MR images. Finally, GTV was defined and drawn on the stereotactic MR image, taking into account the respective contributions of MET-PET and MRI, as well as the anatomic location of the tumor and the functional areas at risk (Fig. 1). The planning target volume (PTV) of SRT-IMRT encompassed the GTV plus a 2-mm

Table 1 Patient characteristics

Characteristic	No. of patients (% or range)
No. of patients	20
Gender	
Male	9 (45)
Female	11 (55)
Age	
Mean (range)	61.3 (42-84 y)
Diagnosis	
NSCLC	10 (50)
Breast cancer	6 (30)
Colon cancer	2 (10)
Renal cell cancer	1 (5)
Other	1 (5)

Abbreviation: NSCLC = non-small cell lung cancer.

Table 2 Metastases characteristics

Characteristic	No. of patients (n=42%)
Gender	
Male	12 (29)
Female	30 (71)
Diagnosis	
NSCLC	23 (55)
Breast cancer	15 (36)
Colon cancer	2 (5)
Renal cell cancer	1 (2)
Other	1 (2)

Abbreviation: NSCLC = non-small cell lung cancer.

margin. SRT-IMRT was performed using HT (helical TomoTherapy; TomoTherapy Inc) in 5 fractions, keeping the dose for PTV at 25 Gy in 10 lesions, 30 Gy in 17 lesions, and 35 Gy in 15 lesions. This dose was prescribed using the 95% isodose line, which covered the PTV.

Follow-up study

For the follow-up study, each patient underwent a series of MET-PET and MRI examinations consisting of a baseline examination prior to SRT-IMRT, at 3 months after SRT-IMRT, and at 6 months following SRT-IMRT. Patients who died after SRT-IMRT were excluded from follow-up at that point. In each case, characteristic changes of MET uptake in lesions post-SRT-IMRT were evaluated quantitatively.

Quantitative evaluation consisted of measurement of the MET uptake value at the PTV. As a normal control, several circular regions of interests with a diameter of 10 mm were located over the gray matter of the contralateral frontal lobe. The lesion vs normal (L/N) ratio was defined as the mean counts of radioisotope per pixel in the lesion of the PTV divided by the mean counts per pixel in the contralateral normal frontal lobe. The L/N ratio within the PTV was calculated prior to SRT-IMRT, at 3 months after SRT-IMRT, and at 6 months after SRT-IMRT. Differences between the 3 groups were examined statistically (see Statistical analysis below).

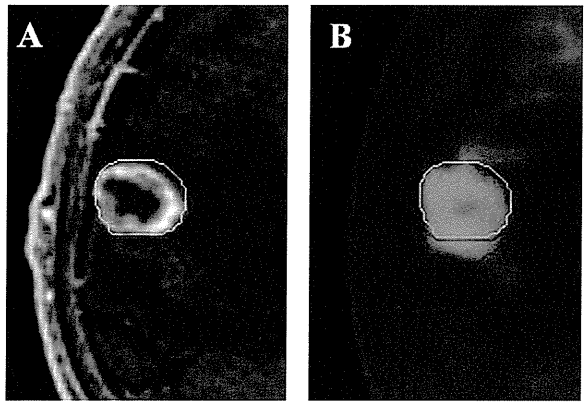

Fig. 1. Dose map of a representative case with MRI (A) and [^{11}C]MET-PET (B). In this case, the lesion's abnormal MET uptake (yellow line) extended beyond the gadolinium-enhanced lesion on MRI (red line). We defined GTV including the lesion of abnormal MET uptake, and the PTV encompassed the GTV-PET plus a 2-mm margin.

On MRI, the tumor responses of SRT-IMRT were classified into 3 types: complete response or partial response (type A), no change (type B), or progressive disease (type C), all determined by the changes in the volume of Gd-DTPA enhancement at 3 months after SRT-IMRT. In each type classified by MRI examination, the L/N ratio of the MET uptake within the PTV was calculated prior to SRT-IMRT, at 3 months after SRT-IMRT, and at 6 months after SRT-IMRT.

A definitive diagnosis of recurrent tumor or radiation necrosis was determined as follows. Recurrence was defined as a case in which pathologic diagnosis was confirmed by tumor resection or biopsy. Diagnosis of radiation necrosis was based on pathologic examination or clinical course. Cases in which lesions showed spontaneous shrinkage or remained stable in size on MRI after a long-term follow-up were assumed to be a delayed tumor response, which could represent radiation necrosis.

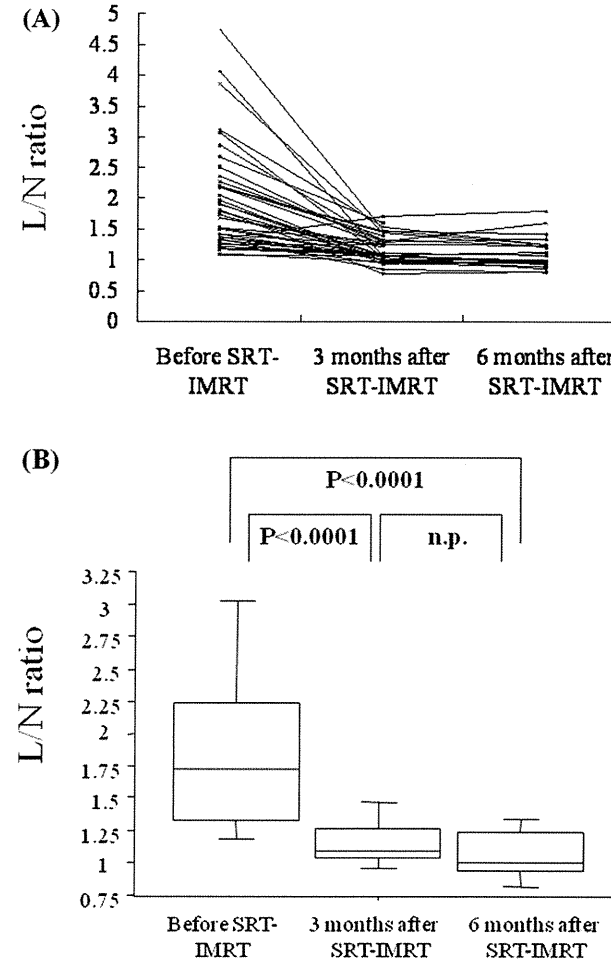

Fig. 2. (A) The ratio of the mean value of [^{11}C]MET uptake to the contralateral normal brain (L/N ratio) plotted at the PTV prior to SRT-IMRT, at 3 months after SRT-IMRT, and at 6 months after SRT-IMRT. (B) Boxplots divide data into 4 qualities. Lower and upper borders of the box represent the 25th and the 75th percentiles, respectively; the middle line represents the median value. The difference in the L/N ratio between the pre-SRT-IMRT group and the 3-month post-SRT-IMRT group was significant ($P<.0001$), as was the difference between the pre-SRT-IMRT group and the 6-month post-SRT-IMRT group ($P<.0001$).